Top Organomet Chem (2020) 66: 279–314
DOI: 10.1007/3418_2020_39

Published online: 31 July 2020

Chiral Metal Nanoparticles for Asymmetric Catalysis

Tomohiro Yasukawa and Shū Kobayashi

Contents

Abstract Metal nanoparticles modified by chiral ligands or chiral polymers, called as "chiral metal nanoparticles," are promising catalysts for asymmetric organic transformations. In this chapter, the class of chiral modifiers is focused to overview advance in the field of metal nanoparticle-catalyzed asymmetric reactions.

T. Yasukawa
Green and Sustainable Chemistry Social Cooperation Laboratory, Graduate School of Science, The University of Tokyo, Bunkyo-ku, Tokyo, Japan

S. Kobayashi (✉)
Green and Sustainable Chemistry Social Cooperation Laboratory, Graduate School of Science, The University of Tokyo, Bunkyo-ku, Tokyo, Japan

Department of Chemistry, School of Science, The University of Tokyo, Bunkyo-ku, Tokyo, Japan
e-mail: shu_kobayashi@chem.s.u-tokyo.ac.jp

Keywords Asymmetric catalysis · Chiral metal nanoparticles · Chiral modifier · Heterogeneous catalysts

1 Introduction

Development of enantioselective catalysis is an important subject as it is an effective process to synthesize target chiral molecules that are further led to useful compounds such as medicines and pesticides [1, 2]. Research using small chiral molecules including metal complexes and organocatalysts as catalysts is a current mainstream in the field of asymmetric catalysis. Numerous homogeneous small molecule catalysts were developed to date, and various transformations were achieved with excellent enantioselectivity. On the other hand, use of chiral molecule-modified surface of metal nanoparticles or supported metal species for asymmetric catalysis was overwhelmingly less developed, though this strategy is attractive because supported metal species are easily separated from a reaction mixture and reused. Indeed, this concept was realized in the early stage of investigations for asymmetric catalysis. In 1956, Akabori et al. reported a Pd catalyst immobilized on silk fibroin fiber for asymmetric hydrogenation of imines as a first example of surface asymmetric catalysis (Scheme 1) [3]. In this reaction, enantioselectivity was still low, and the structure of a chiral modifier was not well-defined. Several years later, the same group reported small chiral molecules such as amino acid- or tartaric acid-modified Raney Ni-catalyzed asymmetric hydrogenations of carbonyl compounds achieving high enantioselectivity (Scheme 1) [4–6]. These studies proved that highly enantioselective catalysis by a chiral ligand-modified metal surface was possible. In 1979, Orito et al. reported asymmetric hydrogenation of methyl pyruvate or

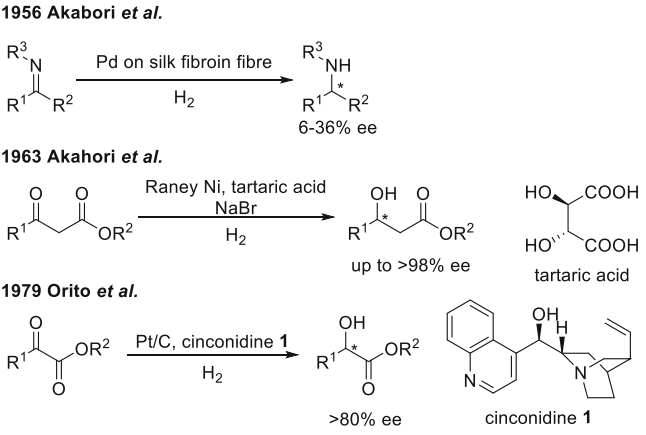

Scheme 1 Early examples of asymmetric catalysis using supported metals and chiral modifiers

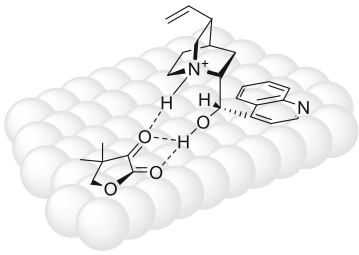

Scheme 2 Proposed reaction mechanism of Orito reaction

methyl benzoylformate catalyzed by cinchonidine **1**-modified Pt on carbon (Scheme 1) [7, 8]. This reaction has attracted interests of many researchers in surface chemistry as well as organic chemistry and catalytic chemistry and was extensively studied even almost 40 years after the discovery to improve the catalyst system and to clarify the reaction mechanism [9–15]. Since there are several excellent review papers that summarize studies of Orito-type reactions and related reactions [16–20], this chapter just briefly introduces it and does not explain more details.

Thanks to these pioneering studies, chiral ligand-modified nanoparticle catalysts, called as chiral nanoparticles in this chapter, were gradually studied, and several reactions including more challenging asymmetric C–C bond-forming reactions could be achieved in high enantioselectivity. Undoubtedly, structures of chiral modifiers are the most important factor, and their role is sometimes not just creation of chiral environments. For example, it was suggested that a cinchonidine modifier in Orito reaction chemisorbed on the metal surface through the interaction of an aromatic moiety and interacted with a substrate on the metal surface to form the individual 1:1 diastereomeric complex through hydrogen bonds (Scheme 2) [21–23]. Therefore, in this chapter, we categorized a class of chiral modifier by structure and overviewed advance of chiral nanoparticle catalysis. Several examples prove a great potential of chiral metal nanoparticles as heterogeneous asymmetric catalyst systems because of their robustness, activity, and unique selectivity. It should be noted that although the true active species was difficult to identify in most cases, several examples described the characteristic nature of chiral nanoparticle catalysts, which show different behavior from the corresponding homogeneous metal complex catalysts. On the other hand, catalytically active species should be carefully discussed since it is possible that a leached homogeneous metal complex is an actual active species. To examine it, several control experiments to evaluate heterogeneity of each catalysis were suggested [24], and we also cover such discussions.

2 Chiral Amine-Modified Nanoparticle Catalysts

Inspired by Orito's asymmetric hydrogenation reaction, cinchona alkaloids derivatives or simpler amines such as 1-(1-naphthyl)ethylamine [25–28] were examined for asymmetric hydrogenation of α-ketoesters [19]. By changing modifier structures,

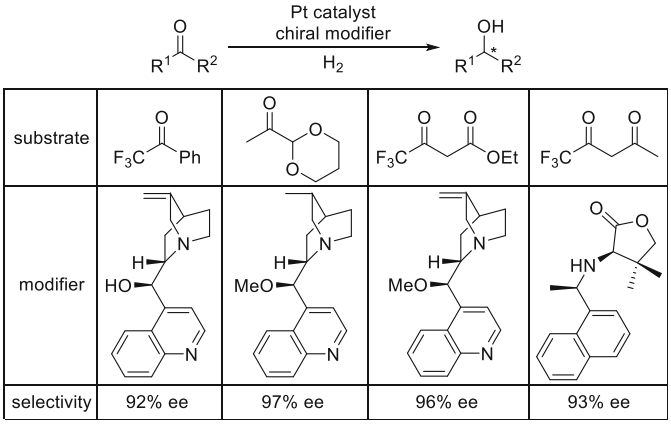

Scheme 3 Representative examples of suitable chiral modifier for Pt-catalyzed asymmetric hydrogenation of various activated ketones

applicable activated ketones were also broaden to a wide variety of activated ketones [29] including α-keto acetals [30], β-ketoesters [31], and trifluoromethyl-substituted ketones [32] (Scheme 3). However, substrate generality in each catalyst system was usually narrow. To expand the scope or develop new reactions, other types of chiral amine modifiers such as chiral diamine and amino acid derivatives were studied for chiral nanoparticle catalyst systems.

2.1 Cinchona Alkaloids and Their Derivatives Modified Nanoparticle Catalysts

In 2015, Wang and Lu et al. reported an alkaloid adsorbed on Cu nanoparticles for electrochemical asymmetric hydrogenation [33]. Cu nanoparticles were prepared by chemical reduction of Cu salts and pressed into a coin to use it as a cathode. In the presence of an alkaloid, cinchonidine **1** or cinchonine, asymmetric reduction of α-ketoesters proceeded in high yields and moderate enantioselectivities (up to 63% ee) under electrochemical conditions. Water was employed as a hydrogen source, and the reaction could be performed under mild conditions. In 2016, the same group improved the system to achieve the same reaction in good enantioselectivities (Scheme 4) [34]. The entrapment of alkaloids within Cu nanoparticles was attempted by the preparation of Cu nanoparticles in an aqueous solution of cinchonidine **1**. The average size of nanoparticles was 100 nm, and they were aggregated into a macroporous solid. EDX spectra and powder XRD pattern indicated cinchonidine **1** was immobilized within small cages of aggregated nanocrystals. Cinchonidine **1** was not washed out in an MeCN/H_2O co-solvent system, and the alkaloid/Cu composite (CD@Cu) could be reused for ten times without loss of activity and selectivity. In 2017, the same group developed bimetallic Pr@Cu nanoparticle

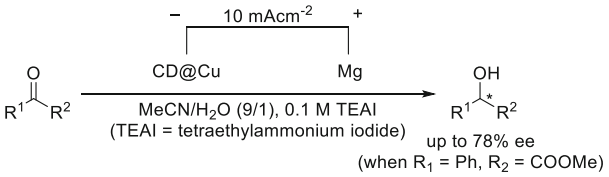

Scheme 4 Alkaloid@Cu nanoparticle composites for electrochemical asymmetric hydrogenation of ketones

Scheme 5 Preparation of Os nanoparticles using a binaphthyl bis-diazonium salt

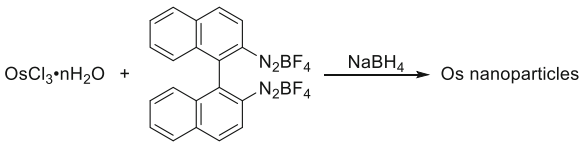

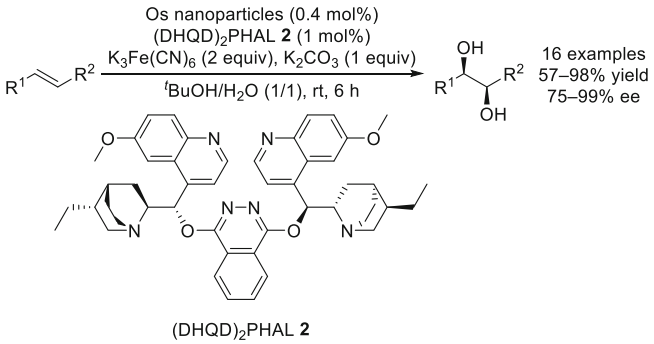

Scheme 6 Bis-cinchona alkaloid-modified Os nanoparticles catalyzed asymmetric dihydroxylation of olefins

cathodes prepared by chemical reduction of Pt salts on Cu nanoparticles for electrochemical asymmetric hydrogenation [35]. The reactions with unactivated ketones were also performed in the presence of cinchonidine **1**; however, poor yields and moderate enantioselectivities were observed.

In 2018, Wu reported bis-cinchona alkaloid-modified Os nanoparticles catalyzed asymmetric dihydroxylation of olefins [36]. Os nanoparticle catalysts were prepared from a binaphthyl bis-diazonium salt as a precursor of stabilizer (Scheme 5). The absence of the diazonium group in the prepared Os nanoparticles was confirmed by FTIR analysis, and the formation of small nanoparticles (1.5–2.0 nm) was confirmed by TEM analysis. Bis-cinchona alkaloid $(DHQD)_2PHAL$ **2** was found to be the best chiral modifier for asymmetric dihydroxylation. The ratio of Os loading and the amount of binaphthyl-based stabilizer were critical for both catalytic activity and enantioselectivity. Many substrates including styrene derivatives and unsaturated carbonyl compounds could be converted to the corresponding diols in high to excellent enantioselectivities (Scheme 6), while nitroolefin and unsaturated nitrile

could not react. The heterogeneous nature of the catalysis was verified by a Hg-poisoning experiment and a hot filtration experiment. And the catalyst could be reused for five cycles without significant loss of activity and aggregation of nanoparticles.

2.2 Chiral Diamine-Modified Nanoparticle Catalysts

Asymmetric hydrogenation of nonactivated aromatic ketones is an atom economical process to prepare chiral alcohols. However, early attempts using chiral ligand-modified heterogeneous catalysts, such as proline-modified Pd/C, cinchona-modified Pt/C, and chiral organotin-modified Pt or Rh, could not achieve high enantioselectivity (~20% ee) [37–40].

In 2007, Zhao et al. reported *R*,*R*-1,2-diphenylethylene diamine ((*R*,*R*)-DPEN)-modified Ru on γ-Al_2O_3-catalyzed asymmetric hydrogenation of acetophenone [41]. A phosphine ligand was additionally employed to effect on the conversion and enantioselectivity, and a relatively high ee (60.5%) was obtained. In the same year, Chen et al. reported asymmetric hydrogenation of aromatic ketones in an ionic liquid using a monophosphine TPPTS [P(*m*-$C_6H_4SO_3Na$)]-stabilized Ru catalyst and chiral diamine **3** as a modifier [42]. $RuCl_3 \cdot 3H_2O$ was reduced by H_2 in the presence of TPPTS as a stabilizer to generate Ru nanoparticles whose size was about 5 nm. The reactions were performed in a co-solvent system with ionic liquid [RMIM]Ts (1-alkyl-3-methylimidazolium *p*-methylphenylsulfonates, R = ethyl, butyl, octyl, dodecyl, hexadecyl), and various aromatic ketones were hydrogenated with high conversions and moderate to high enantioselectivities (Scheme 7). The ionic liquid substituted with the longer alkyl chain decreased enantioselectivity because the Ru catalyst modified with hydrophilic chiral diamine **3** was reduced due to its high solubility in water. This Ru nanoparticle catalyst system was more active than the corresponding metal complex ($RuCl_2(TPPTS)_2$) under the same conditions, although similar high enantioselectivities were obtained by the metal complex. The chiral alcohol products could be separated by extraction with

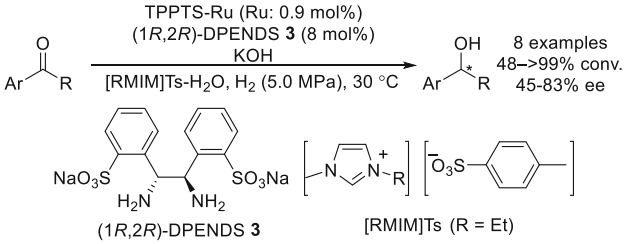

Scheme 7 TPPTS-stabilized Ru in ionic liquids catalyzed asymmetric hydrogenation of aromatic ketones

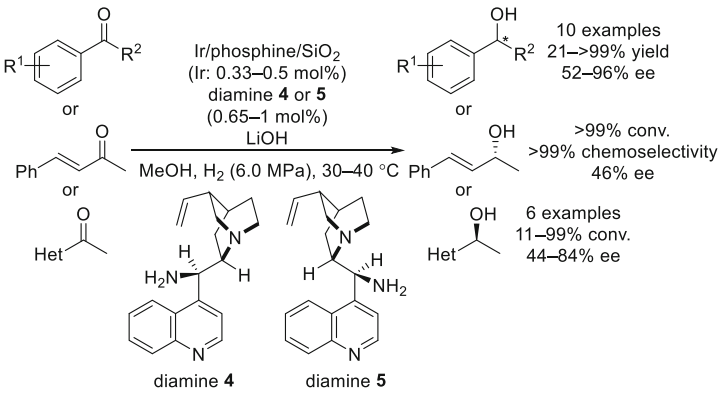

Scheme 8 Chiral diamine-modified Ir/phosphine/SiO_2 catalyzed asymmetric hydrogenation of various ketones

n-hexane, while the catalyst and diamine **4** remained in ionic liquid and water, and they were reused several times.

In 2008, Chen et al. reported a SiO_2-supported Ir catalyst for asymmetric hydrogenation of aromatic ketones [43]. The catalyst was stabilized by an additional phosphine and modified by cinchona alkaloid-derived chiral diamine **4** or **5** to facilitate the reaction with good to excellent enantioselectivities (Scheme 8). Addition of the phosphine is essential for both conversion and enantioselectivity. The corresponding homogeneous Ir/phosphine/diamine catalyst gave low enantioselectivity. The filtering test and mercury-poisoning test also supported the heterogeneous nature of this catalyst system. This catalyst system was applicable for asymmetric hydrogenation of an unsaturated ketone [44] and heteroaromatic methyl ketones (Scheme 8) [45]. In the former reaction, the corresponding allylic alcohol was obtained selectively with moderate enantioselectivity. In the latter reactions, the desired chiral alcohols were obtained with moderate to high enantioselectivities. The same group further investigated asymmetric hydrogenation of acetophenone using the cinchonidine **1**-stabilized Ir particles on SiO_2 with (1*S*,2*S*)-diphenylethylenediamine (DPEN) as a modifier [46]. The synergy between cinchonidine **1** and DPEN improved the reaction rate and enantioselectivity (up to 79.8% ee), while poor results were obtained in the absence of one of them. In 2014, they improved the Ir/PPh_3/SiO_2 system by using monodispersed and silanol-rich silica and 9-amino-(9-deoxy)epicinchonine as a chiral modifier [47]. They demonstrated that silanols enhanced the activity and enantioselectivity via hydrogen bonding between substrates and silanols in the heterogeneous asymmetric hydrogenation of aromatic ketones to achieve excellent enantioselectivities (up to 99.9% ee).

In 2010, Chen et al. reported phosphine-stabilized Ru on γ-Al_2O_3 for asymmetric hydrogenation of aromatic ketones in the presence of chiral diamine **4** as a modifier (Scheme 9) [48]. Under the optimized conditions, various acetophenone and propiophenone derivatives were reduced to the corresponding chiral alcohols with high to excellent enantioselectivities, while low enantioselectivity was observed in

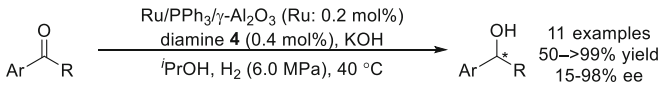

Scheme 9 Chiral diamine-modified Ru/phosphine/Al_2O_3 catalyzed asymmetric hydrogenation of aromatic ketones

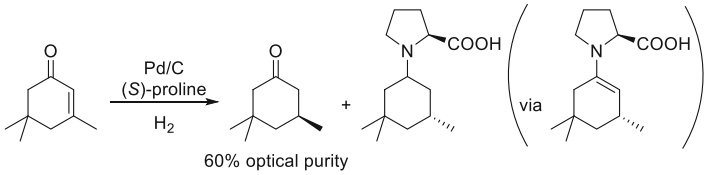

Scheme 10 Pd on carbon with proline catalyzed asymmetric hydrogenation of isophorone

the case that R group was butyl. Control experiments using other modifiers such as cinchonine, cinchonidine **1**, and quinine indicated that the amine group in the 9-position of the modifier was essential.

2.3 Amino Acid-Modified Nanoparticle Catalysts

Direct use of amino acids for chiral induction is attractive because amino acids are readily available chiral sources.

In 1989, Tungler et al. examined asymmetric hydrogenation of unsaturated ketones in the presence of Pd on carbon (Pd/C) with a stoichiometric amount of proline (Scheme 10) [49]. They found that dihydroisophorone can be obtained from isophorone in good enantioselectivity (60% optical purity). Initially, they proposed that enantioselectivity arise from the formation of a proline-/substrate-condensed product that adsorbed on the Pd surface [49, 50]. However, in 2006, Lambert et al. pointed out that this mechanism was not appropriate and the enantioselectivity was resulted from kinetic resolution [51, 52]. In this revised mechanism, initially hydrogenation on a heterogeneous catalyst affords a racemic product, and proline reacts preferentially with one enantiomer to form an enamine, which is further reduced to produce an amine, while an excess of the other enantiomer remains unreacted. Thus, the heterogeneous process is not an enantioselection step in this reaction system. In 2009, Lambert et al. attempted to design surface-tethered chiral modifiers to achieve a truly heterogeneous enantioselective process for the same reaction [53]. Pyrrolidine-contained chiral sulfide ligands that can robustly anchor to Pd nanoparticles were investigated, and the desired products were obtained in good yields and low enantioselectivities (up to 15% ee) in the presence of a catalytic amount of modifier.

In 2006, Török et al. examined proline-modified base-supported Pd catalysts for asymmetric hydrogenation of isophorone [54]. They found that the activity of

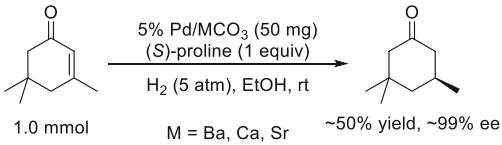

Scheme 11 Proline-modified, base-supported Pd catalyzed asymmetric hydrogenation of isophorone

alkaline earth metal carbonate-supported catalysts produced significant secondary kinetic resolution with excellent enantioselectivity (Scheme 11). The use of basic supports enhanced proline adsorption on the Pd catalyst through an ionic interaction, and a modifier adsorption was a crucial factor in asymmetric hydrogenation. In 2015, the same group investigated aminomethylated polystyrene-supported Pd catalysts for asymmetric hydrogenation of isophorone [55]. In these catalyst systems, a direct enantioselective proline-modified hydrogenation of isophorone occurred without the contribution of a secondary kinetic resolution; however, enantioselectivity was moderate (up to 51% ee).

In 2015, Meemken et al. studied the surface processes occurring at the methanol-Pd catalyst interface using attenuated total reflection infrared spectroscopy to clarify the role of the heterogeneous catalyst in asymmetric hydrogenation of isophorone [56]. They revealed the existence of two competing reaction pathways that were kinetic resolution and Pd-catalyzed stereoselective hydrogenation. The reaction was controlled by these pathways depending on surface coverage of the Pd catalyst.

Use of catalytic amounts of amino acids as chiral modifiers for asymmetric catalysis is also possible.

In 2013, Kunz et al. examined cysteine and its derivatives to functionalize Pt nanoparticles, and asymmetric hydrogenation of 2-butanone was demonstrated [57]. Chiral induction occurred in this system although enantioselectivity was very low (up to 9% ee). In 2015, the same group studied proline-functionalized Pt nanoparticles supported on alumina (PRO-Pt/Al_2O_3) for asymmetric hydrogenation of acetophenone [58]. Phenyl-1-ethanol was selectively obtained with low enantioselectivity (14% ee), while unprotected Pt nanoparticles gave a mixture of phenyl-1-ethanol and cyclohexyl-1-ethanol. An enhanced rate toward phenyl-1-ethanol was found for proline-functionalized Pt nanoparticles in comparison with unprotected ones. They also investigated the effect of particle size on the asymmetric catalytic properties of supported proline-functionalized Pt nanoparticles [59]. An asymmetric hydrogenation of ethylacetoacetate was chosen as a model, and moderate enantioselectivity (up to 34% ee) was obtained. The enantioselectivity was not altered by the particle size, suggesting that the selectivity was primarily determined by the ligand-reactant interaction that worked between the carbonyl group of the substrate and the N–H group of proline. On the other hand, the activity was determined by the particle size.

In 2017, Kunz et al. applied PRO-Pt/Al_2O_3 for asymmetric hydrogenation of β-ketoesters [60]. The effect of substituents was studied, and good enantioselectivity (73% ee) was obtained when R^1 group was bulky *tert*-butyl group (Scheme 12). In 2018, the same group reported further examination of the effects of amino acids for the same reaction system [61]. Various combinations of substrates and amino acids

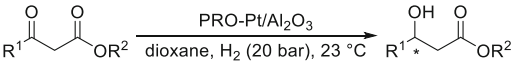

R^1	Me	Et	^{n}Pr	^{n}Bu	^{i}Pr	^{t}Bu	Me	Me	Me	Me	Me
R^2	Me	Me	Me	Me	Me	Me	Et	^{n}Pr	^{n}Bu	^{i}Pr	^{t}Bu
ee (%)	39	55	60	64	67	73	39	40	42	39	35

Scheme 12 PRO-Pt nanoparticles catalyzed asymmetric hydrogenation of β-ketoesters

Scheme 13 Amino acid-functionalized Pt nanoparticles catalyzed asymmetric hydrogenation of β-ketoesters

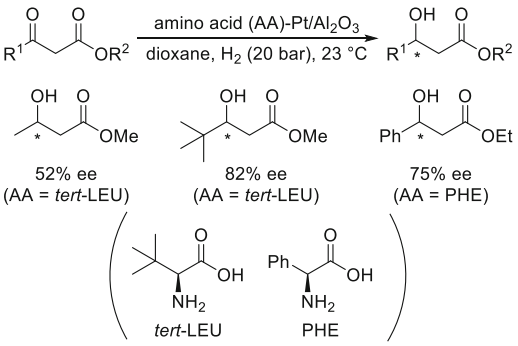

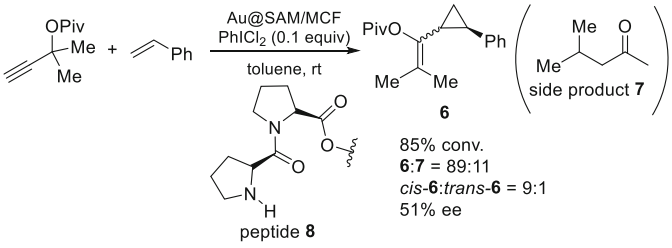

Scheme 14 Au@SAM/MCF-17 catalyzed asymmetric intermolecular cyclopropanation

as chiral ligands for nanoparticles were screened to enhance enantioselectivity. High enantioselectivity (up to 82% ee) was observed when bulky substituents were introduced to both substrate and chiral ligand (Scheme 13). Experimental results and simulations suggested that the NH group and the COOH group of the ligand might interact with two carbonyl groups of the reactant.

In 2013, Toste and Somorjai et al. developed Au nanoparticle catalysts immobilized on a chiral self-assembled monolayer (SAM) on the surface of a mesoporous silica support for asymmetric cyclopropanation reactions [62]. Amino acids were attached to the surface of the mesoporous silica (MCF-17) through the OH functionalities to create a chiral SAM. Au ions were introduced to the support, and the encapsulated Au ions were reduced to nanoparticles by exposure to H_2 atmosphere. The obtained Au nanoparticles catalyst (Au@SAM/MCF) was employed in the intermolecular cyclopropanation reaction of styrene with propargyl pivalate (Scheme 14). In order to generate real active Au catalysts within the

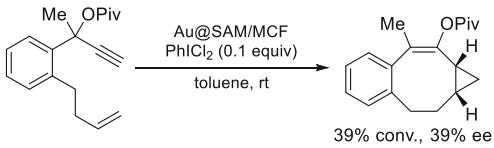

Scheme 15 Au@SAM/MCF-17 catalyzed asymmetric intramolecular cyclopropanation

heterogeneous support, 0.1 equiv. of an oxidizer was used for the reaction. The desired product **6** was obtained in good diastereoselectivity and moderate enantioselectivity, when peptide **8** was immobilized on the surface of the mesoporous silica. The corresponding homogeneous system using $AuCl_3$ and unsupported diproline in the intermolecular reaction showed low yield and no enantioselection. While no leaching of Au complexes to a solution phase was confirmed by ICP analysis, in situ near-edge X-ray adsorption fine structure (NEXAFS) measurements under the reaction conditions proved the formation of Au(III) ions as active species, which were generated from Au(0) nanoparticles by oxidation with an externally added oxidant, $PhICl_2$. The same catalyst could be also used for the asymmetric intramolecular cyclopropanation reactions, although moderate conversion and enantioselectivity were observed (Scheme 15). Although the enantioselectivity was not enough high, the advantages of the surrounding chiral SAM for the formation of a mesoscale enantioselective catalyst were noted.

3 Chiral Phosphine-Modified Nanoparticle Catalysts

Chiral phosphorus ligands have played an important role in the development of asymmetric catalysis. Since early investigations of asymmetric hydrogenation in the period of 1970–1980, thousands of efficient chiral phosphine ligands with diverse structures have been developed [63–65]. They have been extensively utilized in both academic research and industry for not only asymmetric hydrogenation but also asymmetric C–C bond-forming reactions. Inevitably, chiral phosphines were examined as a modifier for metal nanoparticles, and various asymmetric catalysis including asymmetric C–C bond-forming reactions were developed. This section also covered phosphine modifiers that contain amine or hydroxy group as a coordination site. Since there are many types of chiral phosphine modifiers, subsections were categorized by type of reactions.

3.1 Asymmetric Hydrogenation

In 2009, Morris et al. developed chiral Fe complex **9** with a PNNP-type tetradentate ligand-catalyzed asymmetric transfer hydrogenation of ketones (Scheme 16) [66]. They found that these Fe pre-catalysts showed an induction period during catalysis [67], and in 2012, their further mechanistic investigations strongly

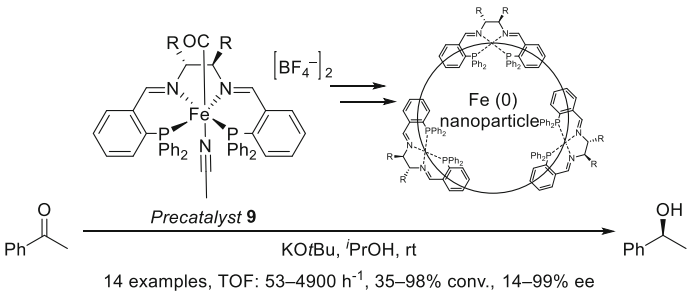

Scheme 16 Chiral Fe nanoparticles as proposed active species catalyzed asymmetric transfer hydrogenation of ketones

Scheme 17 Chiral Fe species catalyzed asymmetric hydrogenation of aromatic ketones

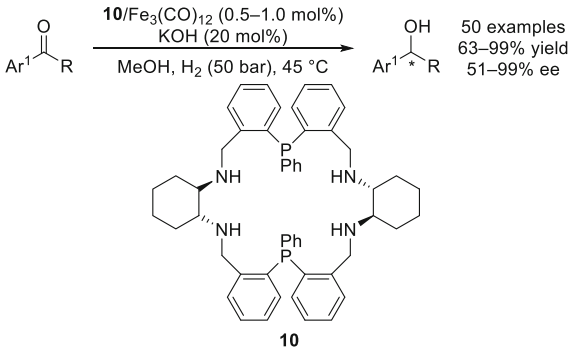

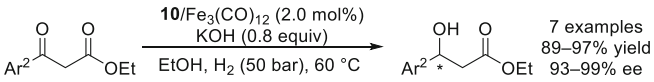

Scheme 18 Chiral Fe species catalyzed asymmetric hydrogenation of β-ketoesters

suggested PNNP ligand-modified Fe(0) nanoparticles as the active species in the reaction system [68, 69]. STEM analysis showed that Fe nanoparticles were approximately 4.5 nm in diameter, SQUID analysis revealed that the catalytic mixture contained a superparamagnetic species, and XPS analysis confirmed the formation of Fe(0) species. Poisoning test using PMe_3 completely inhibited the reaction, and the result of the reaction with a polymer-immobilized substrate also supported that Fe nanoparticles were active species. This is a rare example of highly active chiral zerovalent nanoparticles not based on precious metals. According to DFT studies, the process, in which the pre-catalyst **9** loses its acetonitrile ligand and is reduced to an Fe(0) species, is energetically favorable [70].

In 2014, Gao et al. reported asymmetric hydrogenation reactions catalyzed by chiral Fe catalysts [71]. An iron carbonyl complex with chiral 22-membered macrocyclic ligand **10** was found to be effective for asymmetric hydrogenation of aryl ketones including heteroaromatics (Scheme 17) and β-ketoesters (Scheme 18) under

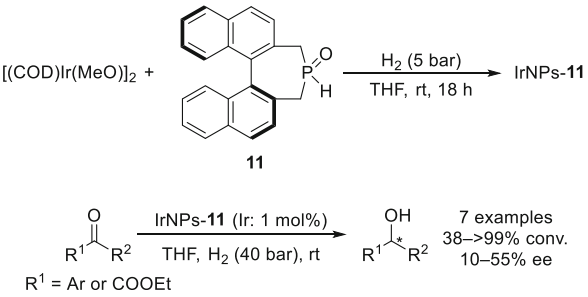

Scheme 19 Chiral iridium nanoparticles catalyzed asymmetric hydrogenation of ketones

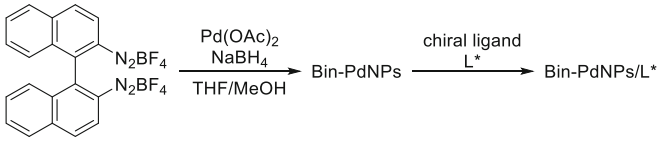

Scheme 20 Preparation of Pd nanoparticles using a binaphthyl bis-diazonium salt

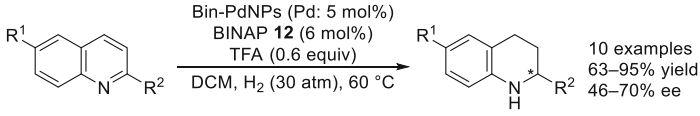

Scheme 21 Bin-PdNPs catalyzed asymmetric hydrogenation of quinolines

basic conditions. Broad substrate generality was achieved with good to excellent enantioselectivities. Several mechanistic observations indicated that active species in the Fe catalyst system might be heterogeneous with **10**-modified Fe particles. For examples, dynamic light scattering confirmed the existence of Fe particles, and a significant poisoning effect was observed.

In 2016, Leeuwen et al. reported a chiral secondary phosphine oxide-modified Ir nanoparticle catalyst for asymmetric hydrogenation of ketones [72]. Ir nanoparticles (IrNPs-**11**) were prepared by H_2 reduction of an Ir salt in the presence of 0.5 eq. (based on Ir) of enantiopure phosphine oxide **11** (Scheme 19). The non-supported IrNPs-**11** could catalyze asymmetric hydrogenation of aromatic ketones and ethyl pyruvate to afford the corresponding alcohols in low to moderate enantioselectivities (Scheme 19). A mercury-poisoning experiment led to the complete inhibition of the reaction, indicating that the nanoparticles were responsible for the catalysis.

In 2017, Wu et al. reported chiral diphosphine-modified Pd nanoparticle catalysts for asymmetric hydrogenation of N-heteroaromatics [73]. Pd nanoparticle catalysts were prepared from a binaphthyl bis-diazonium salt as a precursor of a stabilizer and were modified by chiral ligands (Scheme 20). Chiral Pd nanoparticles modified by 2,2′-bis(diphenylphosphino)-1,1′-binaphthyl (BINAP) **12** were effective for asymmetric hydrogenation of quinolines in the presence of an acid, and the corresponding tetrahydroquinolines were obtained in moderate to good enantioselectivities (Scheme 21). When the chiral ligand was changed to 8H-BINAP **13**, the catalyst

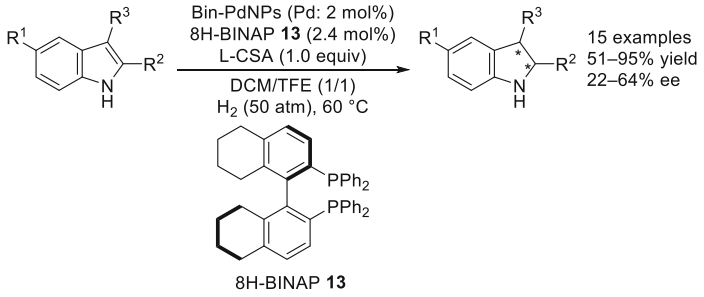

Scheme 22 Bin-PdNPs catalyzed asymmetric hydrogenation of indoles

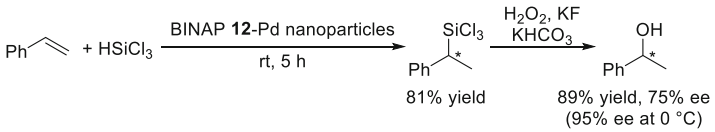

Scheme 23 BINAP **12**-Pd nanoparticles catalyzed asymmetric hydrosilylation of styrene

system could be applied to asymmetric hydrogenation of indoles with moderate enantioselectivities (Scheme 22).

3.2 Asymmetric Hydrosilylation

Asymmetric hydrosilylation is a powerful method to synthesize chiral alcohols from prochiral compounds such as ketones and olefins, because the C–Si bonds can be easily oxidized and O–Si bonds can be easily hydrolyzed to afford the corresponding alcohols [74]. In 2003, Fujihara et al. reported BINAP **12**-modified Pd nanoparticles catalyzed asymmetric hydrosilylation of styrene (Scheme 23) [75]. Chiral Pd nanoparticles were prepared from K_2PdCl_4 by the reduction with $NaBH_4$ in the presence of BINAP **12**, and a small size of nanoparticles with narrow dispersity (2.0 ± 0.5 nm) was confirmed by TEM analysis. The BINAP **12**-stabilized Pd nanoparticles could catalyze asymmetric hydrosilylation of styrene, and an excellent enantioselectivity was observed, while the corresponding BINAP **12**-Pd complex could not catalyze this reaction under the same reaction conditions.

In 2007, Kantam et al. reported nanocrystalline copper oxide (nano-CuO), which possessed high surface area (136 m^2/g) and a small particle size (7–9 nm), catalyzed asymmetric hydrosilylation of aromatic ketones [76]. In the presence of BINAP **12** as a chiral modifier, the reactions with phenylsilane proceeded well for various aromatic ketones to afford the corresponding chiral alcohols in good to excellent enantioselectivities after workup with TBAF (Scheme 24). The catalyst could be reused for four times without significant loss of activity and selectivity. No reaction occurred in the filtrate obtained after removal of the solid catalyst indicating that the

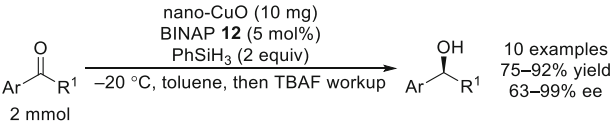

Scheme 24 Nano-CuO with BINAP **12** catalyzed asymmetric hydrosilylation of aromatic ketones

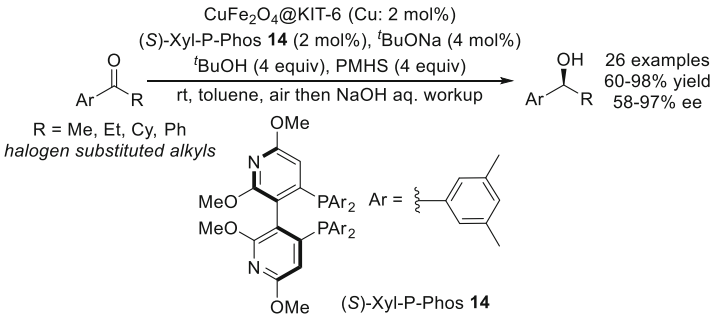

Scheme 25 $CuFe_2O_4$@KIT-6 with Xyl-P-Phos **14** catalyzed asymmetric hydrosilylation of aromatic ketones

active species were not leached out. XPS analysis revealed that both +2 and +1 oxidation states of Cu were observed after treatment with BINAP **12** and silane, while the fresh catalyst and the used catalyst showed the peak corresponding to +2 oxidation state. In 2009, the same group reported copper ferrite nanoparticles ($CuFe_2O_4$) for asymmetric hydrosilylation of aromatic ketones with polymethylhydrosiloxane (PMHS) as an inexpensive, nontoxic, and air-stable hydride source [77]. In the presence of the nanoparticles and BINAP **12**, various aromatic ketones and ketoesters were converted to the corresponding alcohols in moderate to excellent enantioselectivities at room temperature. The Cu catalyst could be magnetically separable and could be reused for three times without significant loss of activity and selectivity.

In 2014, Wu and Shi et al. developed $CuFe_2O_4$ nanoparticles supported on mesoporous silica (KIT-6) matrix for asymmetric hydrosilylation of aromatic ketones [78]. The reaction with PMHS proceeded in the presence of Xyl-P-Phos **14** as a chiral modifier at room temperature under air, and wide substrate generality including halo-substituted alkyl aryl ketones was demonstrated with good to excellent enantioselectivities (Scheme 25). The magnetically separated catalyst could be reused for four cycles; however, the enantioselectivity decreased slightly. Nitrogen sorption analysis indicated that the specific surface and the pore volume area decreased after the catalytic reaction. TGA analysis showed that more than 8 wt% organic species were recorded for the reused catalyst. These results indicated that the chiral ligands were strongly bound to the nanoparticles, and they were difficult to wash out.

3.3 Asymmetric C–C Bond-Forming Reaction

3.3.1 Palladium Nanoparticle Catalysis

In 2001, Kobayashi et al. developed a Pd(0) catalyst encapsulated by polystyrene (MC Pd(PPh_3)), which was successfully used for a catalytic asymmetric allylation reaction (Scheme 26) [79]. In the presence of chiral phosphine-oxazoline **15**, the allylated adduct was obtained in high yield with high enantioselectivity.

In 2004, Gómez, Philippot, and Chaudret et al. reported asymmetric allylic alkylation reactions catalyzed by colloidal Pd nanoparticles stabilized with chiral diphosphite **16** derived from a xylose backbone (Scheme 27) [80]. The catalytic performance of a molecular Pd complex prepared in situ from $[Pd(C_3H_5)Cl]_2$ with **16** was compared with that of nanoparticles (Scheme 28). In the case of a nanoparticle catalyst system, the reaction mainly proceeded with only one of the enantiomers of substrate **20**, and a very efficient kinetic resolution was demonstrated. On the other hand, no kinetic resolution was observed in the presence of the molecular complex.

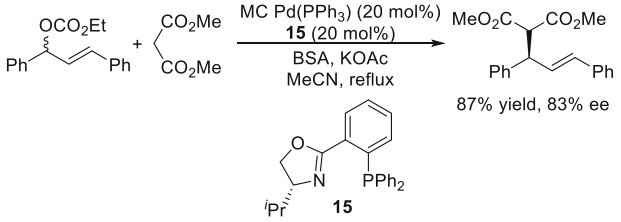

Scheme 26 Microencapsulated (MC) Pd-catalyzed asymmetric allylation

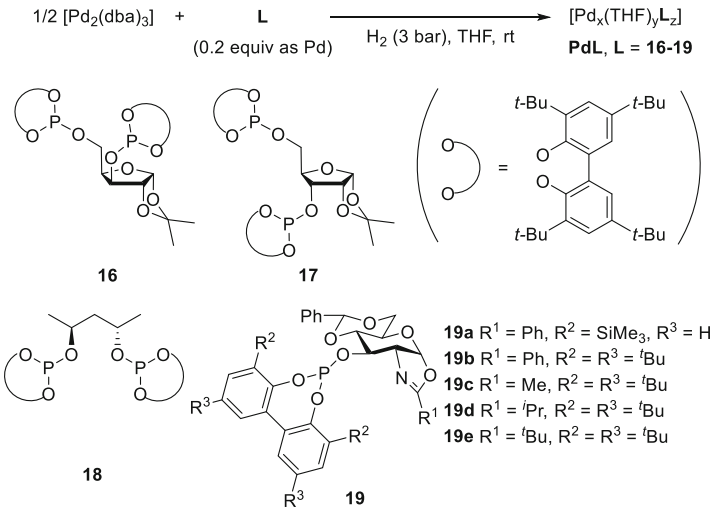

Scheme 27 Preparation of chiral diphosphite ligands stabilized Pd nanoparticles

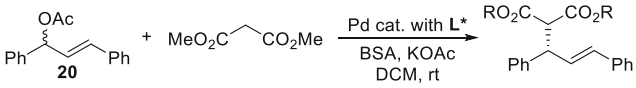

Pd nanoparticle **16**: ~60% conv., 97% ee (recovered **20**: 89% ee)
molecular complex: ($[Pd(C_3H_5)Cl]_2$ + **16**): 95% conv., 90% ee

Scheme 28 Chiral diphosphite ligand **16**-based Pd catalysts for asymmetric allylic alkylation

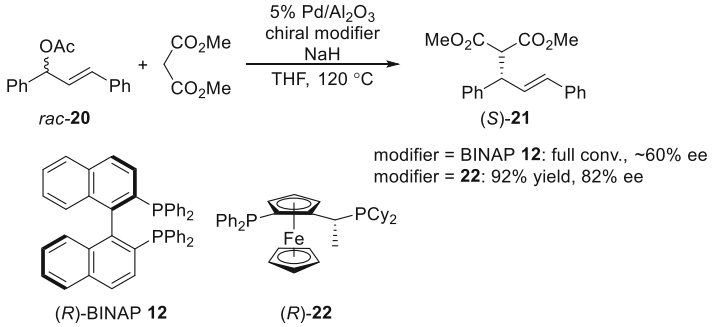

Scheme 29 Chiral phosphine-modified Pd/Al_2O_3 catalyzed asymmetric allylic alkylation

In 2007, the same group reported detailed studies of this reaction with different chiral modifiers and substrates [81]. Three types of ligands **16**–**18** were examined, and Pd-**16** and Pd-**18** could give the product in excellent enantioselectivities. On the other hand, Pd-**17** easily decomposed into metal complex species and could not induce high enantioselectivity, while Pd-**16** and Pd-**18** did not decompose. Alkyl-substituted allyl acetates were not alkylated by using Pd-**16** or Pd-**18**, while the corresponding metal complex catalyst systems gave high conversions. In 2008, Diéguez, Gómez, and Leeuwen et al. reported chiral oxazolinyl-phosphite ligands **19a**–**19e**- modified Pd nanoparticle systems for the same reaction [82]. The nature of active species was studied using continuous-flow membrane reactor (CFMR), transmission electron microscope (TEM) observations, classical poisoning experiments, and kinetic measurements. Those studies proved the molecular nature of the truly active species that was leached out from the catalyst.

Heterogeneous Pd nanoparticle catalysts with chiral modifiers were also examined for asymmetric allylic alkylation. In 2005, Felpin and Landais reported the combination of Pd/C and (*R*)-BINAP **12** for the reaction of racemic **20** with diethylmalonate in water, and high enantioselectivity (80% ee) was achieved, while the yield was low (21%) [83]. In 2007, Baiker et al. reported BINAP **12**-modified Pd/Al_2O_3 catalyst systems for the reaction of racemic **20** with the sodium salt of dimethylmalonate (Scheme 29) [84]. Pd/Al_2O_3 treated under hydrogen gas showed good chemoselectivity (94%) and moderate enantioselectivity (~60% ee) in the presence of BINAP **12**. The enantioselectivity of this system was independent on reaction temperatures (60 and 120°C), while the corresponding homogeneous complex catalyst showed poor enantioselectivity to give the opposite enantiomer of the

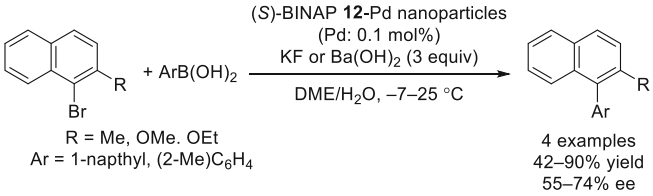

Scheme 30 BINAP **12**-modified Pd nanoparticles catalyzed asymmetric Suzuki-Miyaura coupling

product (*R*-**21**) at 60°C or above. In 2008, the same group improved the enantioselectivity of this reaction to 82% ee by changing the chiral modifier to ferrocenyl phosphine ligand **22** (Scheme 29) [85]. No temperature dependence on the enantioselectivity was observed again (at 60 and 120°C). In the corresponding homogeneous metal complex system, the same enantiomer of the product (*S*-**21**) was produced; however, the enantioselectivity was decreased by increasing the reaction temperature from 85% ee at 60°C to 55% ee at 120°C. In 2010, the same group reported detailed studies of the nature of the active species in Pd/Al_2O_3-BINAP **12** system and emphasized heterogeneity [86]. The oxidation state of Pd was elucidated by in situ X-ray absorption near-edge structure (XANES) analysis in a reaction mixture. Partially oxidized surface of Pd nanoparticles could be reduced by the reaction components, such as the solvent and sodium dimethyl malonate to maintain their reduced state during the reaction without Pd leaching. In contrast, the addition of a chlorinated solvent, such as chloroform, favored dissolution of metallic Pd to form homogeneous catalyst species.

In 2008, Fujihara et al. reported chiral bisphosphine-modified chiral Pd nanoparticles and their application to asymmetric Suzuki-Miyaura coupling reactions (Scheme 30) [87]. Pd nanoparticles were prepared by reduction of K_2PdCl_4 with $NaBH_4$ in the presence of a chiral phosphine. Several bisphosphine ligands were tested for the coupling reactions, and (*S*)-BINAP **12** was found to be the best chiral modifier in terms of activity, enantioselectivity, and stability of chiral Pd nanoparticles to afford axially chiral biaryl compounds in good enantioselectivities at low temperature (−7 to 25°C).

In 2009, Yamashita et al. reported that BINAP **12**-modified bimetallic Fe/Pd nanoparticles with core-shell structure catalyzed asymmetric Suzuki-Miyaura coupling reaction [88]. The catalyst worked for the coupling reaction between 1-bromo-2-methoxynaphthalene and 2-naphthyl boronic acid with moderate enantioselectivity (up to 48% ee). The nanoparticles were easily recovered by magnet and could be reused with keeping identical enantioselectivity without an external addition of a chiral modifier. The hot leaching test was conducted, and the reaction hardly occurred in the filtrate after removal of the catalyst.

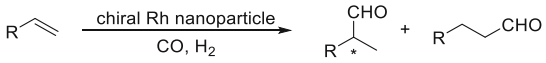

Scheme 31 Chiral Rh nanoparticles catalyzed asymmetric hydroformylation

3.3.2 Rh Nanoparticle Catalysis

Asymmetric hydroformylation of olefins using inexpensive syngas is a useful method to synthesize optical active aldehydes. While a chiral Rh complex was often used for this reaction [89] and Rh nanoparticles were also studied for non-asymmetric hydroformylation [90], development of chiral Rh nanoparticle systems for asymmetric hydroformylation is still a challenging topic (Scheme 31).

In 2000, Anderson et al. reported chiral diphosphine ligand-modified $Rh/SiO_2 \cdot Al_2O_3$ catalyzed asymmetric hydroformylation of styrene although enantioselectivity was low (up to 9% ee) [91]. In 2006, Li et al. reported asymmetric hydroformylation of styrene or vinyl acetate catalyzed by BINAP **12**-modified Rh/SiO_2 [92]. A good enantioselectivity (up to 72% ee) and 100% selectivity of a branched aldehyde for the hydroformylation was obtained; however, the conversion was poor (<10%). In 2008, the same group reported a different method to prepare modified Rh nanoparticles by one-pot chemical reduction of aqueous rhodium chloride dispersed in toluene in the presence of amphiphilic tetraoctylammonium bromide (TOAB) and (*R*)-BINAP **12** [93]. These BINAP **12**-modified Rh nanoparticles could be also immobilized on SiO_2 in vacuum by adsorption; however, no significant improvement of catalytic performance was observed. In 2008, Axet, Claver, and Philippot reported asymmetric hydroformylation of styrene using colloidal Rh nanoparticles modified with carbohydrate-derived diphosphite ligands [94]. With the addition of an excess amount of the ligand, high conversion, high regioselectivity, and moderate enantioselectivity (31% ee) were observed. In situ high-pressure (HP) NMR spectroscopic studies under catalytic conditions in the presence of chiral Rh nanoparticles led to detection of the hydridorhodium diphosphite complex $[RhH(CO)_2(L)]$. These results indicated that metal complex species generated from nanoparticles also worked as active species. Given that the difference of enantioselectivity between the molecular complex system and the nanoparticle system, a possibility that some activity comes from nanoparticles cannot be excluded. In 2018, Trzeciak et al. reported DNA-stabilized Rh nanoparticle catalysts for asymmetric hydroformylation [95]. In the presence of BINAP **12**, asymmetric hydroformylation of vinyl acetate proceeded to afford the corresponding branched product in moderate yield (~30%) and moderate enantioselectivity (49% ee). The analyses of the organic phase of the post-reaction mixtures by ^{31}P NMR and IR indicated that a hydridorhodium complex, $HRh(CO)_2$(BINAP **12**), formed when Rh nanoparticles were dissolved under hydroformylation conditions.

Another way to utilize carbon monoxide for organic synthesis is Pauson-Khand reaction that is a [2 + 2 + 1] cycloaddition among an alkyne, an alkene, and carbon monoxide to construct cyclopentenone skeleton. In 2005, Chung et al. reported charcoal-immobilized Co/Rh heterobimetallic nanoparticles catalyzed asymmetric

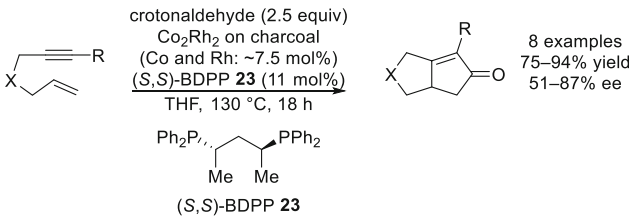

Scheme 32 Chiral diphosphine **23**-modified Co/Rh on charcoal catalyzed asymmetric Pauson-Khand reactions

Pauson-Khand-type reactions with a chiral diphosphine modifier [96]. Chiral diphosphine **23-**modified Co/Rh catalysts worked well for the reactions of several enynes with crotonaldehyde as a source of carbon monoxide proceeded, and the corresponding bicyclic cyclopentenones were obtained in high yields with moderate to good enantioselectivities (Scheme 32). The catalyst could be reused with the addition of a new chiral modifier in each run for five times without significant loss of yield and enantioselectivity. ICP-AES analysis of the reaction mixture obtained after three cycles detected 3.9 ppm of Co and 0.3 ppm of Rh species; however, the results of mercury-poisoning test supported heterogeneous nature of active species as Hg (0) completely eliminated further catalysis after the addition of Hg(0) to the reaction mixture.

3.4 Miscellaneous

In 2018, Xu et al. reported chiral Cu nanoparticles catalyzed desymmetrization of pyrazolone-derived bisalkynes through catalytic asymmetric Huisgen [3 + 2] cycloaddition [97]. CuF_2 was initially used for the screening of chiral ligands, and Tao-Phos **24** was found to be the best ligand. Several Cu salts were then examined, and Cu_2O whose particle size was ~20 nm gave also similar good performance with that of CuF_2. A Tao-Phos **24**-Cu nanoparticle system worked for several aromatic substrates with good to high enantioselectivities (Scheme 33). The nonlinear relationship between enantiopurity of the ligand and the product was observed. In contrast to a CuF_2 system, ESI-MS analysis in the Cu_2O system could not detect the corresponding Cu complex-derived peak indirectly suggesting that the formation and absorption of Cu/Tao-Phos **24** complex on the surface of nano Cu_2O could be recognized. A hot filtration test also supported the stable adsorption of Tao-Phos **24** on nano Cu_2O.

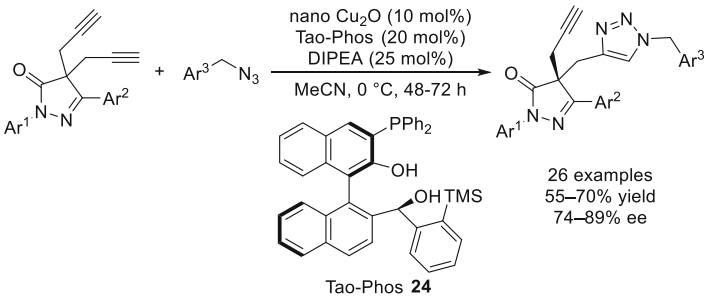

Scheme 33 Tao-Phos **24**-Cu nanoparticles catalyzed asymmetric Huisgen alkyne-azide cycloaddition of bisalkynes

4 Chiral N-Heterocyclic Carbene-Modified Nanoparticle Catalysts

N-Heterocyclic carbenes (NHCs) have been widely studied not only as ligands for metal complexes and organocatalysts but also as stabilizers for metal nanoparticles because of their strong surface binding [98, 99].

In 2010, Glorius et al. reported the first successful application of chiral NHC for metal nanoparticle-catalyzed asymmetric reactions [100]. Chiral NHC **25** bearing hydroxy groups was utilized to modify Pd nanoparticles supported on magnetite (Fe_3O_4/Pd) (Scheme 34), and this system showed good catalytic performance for asymmetric α-arylation of ketones with aryl halides (Scheme 35). Various types of cyclic ketones and aryl halides could be employed to afford the corresponding α-arylated ketones in moderate enantioselectivities. Intramolecular α-arylation reactions of amide substrates could also proceed smoothly, and relatively high enantioselectivities were observed (Scheme 36). In the latter reaction (when X = Cl, R^1 = Bn, R^2 = Et, Ar = Ph), the corresponding homogeneous Pd complex catalyst system $(Pd(allyl)Cl)_2$ and chiral NHC **25**) gave a poor result (32% yield, 23% ee), indicating that an activity principle of the chiral nanoparticle system is different from that of a homogeneous complex system. The heterogeneous nature of the active species was further confirmed by a hot filtration test, a mercury-poisoning test, and trace-metal analysis by ICP-OES. The paramagnetic catalyst could be recovered using a magnet and reused for five cycles without significant loss of activity and selectivity.

Several characterization of the obtained NHC-modified Pd catalyst (Fe_3O_4/Pd/**25**) was conducted. XPS analysis confirmed that zero valency of Pd was maintained even after the surface modification. Attenuated total reflection infrared spectroscopy (ATR-IR) analysis could detect the NHC-modified surface by comparison of the spectra obtained from the free salt **25** and that of Fe_3O_4/Pd/**25**, and marked differences were observed. Different BET surfaces were obtained for Fe_3O_4, Fe_3O_4/Pd, and Fe_3O_4/Pd/**25**.

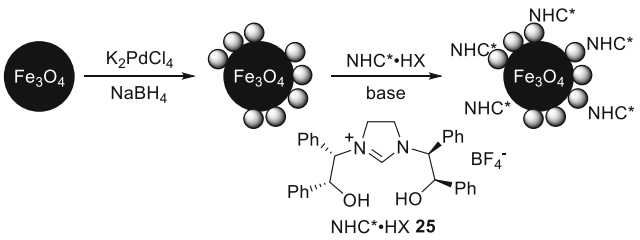

Scheme 34 Preparation of chiral NHC **25** modified Fe_3O_4/Pd nanoparticles

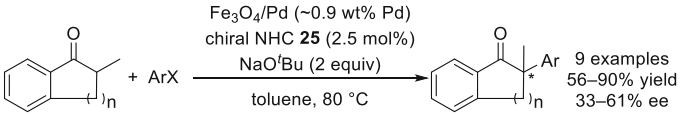

Scheme 35 Chiral NHC **25**-Pd nanoparticle catalyzed asymmetric α-arylation of ketones with aryl halides

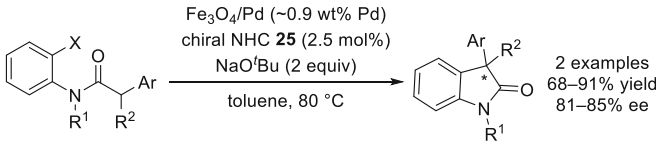

Scheme 36 Chiral NHC **25**-Pd nanoparticle catalyzed intramolecular asymmetric α-arylation of amides with aryl halides

The same group examined a combination of Fe_3O_4/Pd and quinine as a chiral modifier for the asymmetric α-arylation reaction [101]. Good yields and enantioselectivities were obtained; however, a mercury-poisoning test and a filtration test indicated that the nature of the active species was not heterogeneous. These results emphasized the important role of NHC as a modifier for both stability and activity of the Pd nanoparticle catalysts.

In 2011, Glorius et al. developed Fe_3O_4-supported chiral NHC-based catalysts [102]. Molecular catalyst **27** was prepared by complexation of supported chiral NHC **26** with $Pd(OAc)_2$, while Pd nanoparticle catalyst **28** was prepared by the reduction of K_2PdCl_4 in the presence of the same supported NHC **26** (Scheme 37). The oxidation states of Pd in these catalysts were determined by XPS analysis to confirm the formation of a Pd complex or Pd(0) nanoparticles. These two heterogeneous Pd catalysts were applied to the asymmetric allylation of 4-nitrobenzaldehyde with allyltributyltin, and the results were compared (Scheme 38). The nanoparticle catalyst **28** gave better results for both yield and enantioselectivity, and surprisingly, the product was obtained with the opposite absolute configuration to that obtained with the molecular catalyst **27**.

In 2018, Toste and Somorjai et al. reported heterogeneous Au nanoparticle catalysts with NHC ligands prepared by a strategy of supported dendrimer-

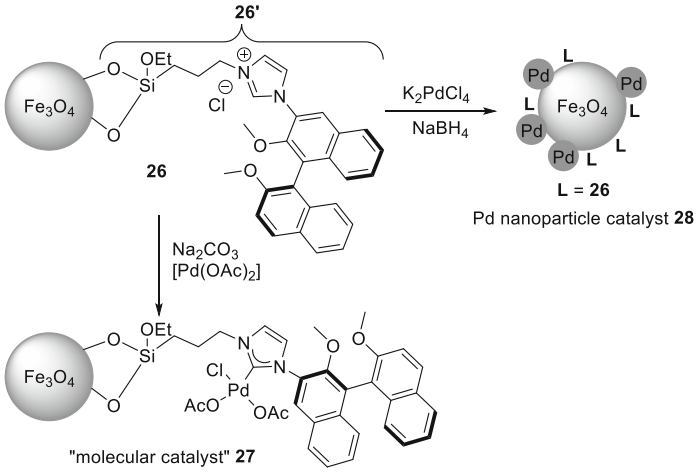

Scheme 37 Preparation of a molecular catalyst and a Pd nanoparticle catalyst from Fe_3O_4-supported chiral NHC **26**

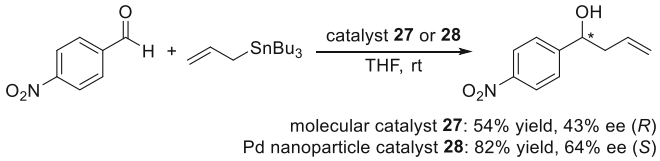

Scheme 38 Chiral NHC-Pd nanoparticle catalyzed asymmetric allylation of 4-nitrobenzaldehyde with allyltributyltin

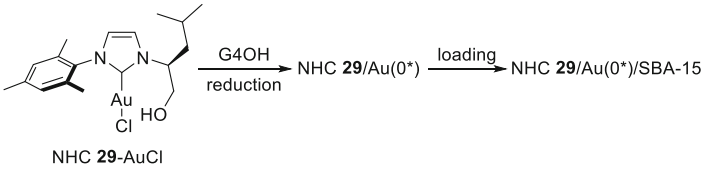

Scheme 39 Preparation of supported Au nanoparticles with NHC ligand **29**

encapsulated metal clusters (DEMCs) [103]. L-Amino acid-derived chiral NHCs with a hydroxyl group were chosen as a modifier. The hydroxy group was expected to strengthen interactions of the NHC-ligated Au nanoparticle with SBA-15 and to facilitate proto-deauration that had been postulated to be turnover-limiting step [104]. Au nanoparticles were prepared from a chiral NHC-Au complex in the presence of a dendrimer (G4OH) that enhances the stability of the nanoparticles to aggregation, and they were further loaded on SBA-15 (Scheme 39). XPS, XANES, and time-of-flight secondary ion mass spectrometry (ToF-SIMS) analysis revealed that the Au nanoparticles prepared from the NHC complex were coated with monolayers of Au(I) species, presumably NHC-Au(I) complexes.

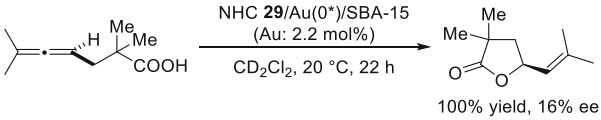

Scheme 40 Chiral NHC **29**-Au nanoparticle catalyzed asymmetric lactonization

These chiral Au nanoparticle catalysts were applied to asymmetric lactonization of allene-carboxylic acids (Scheme 40). Eleven types of chiral NHCs were screened, and the desired products were obtained in quantitative yields and maximally 16% ee. Although the enantioselectivity was low, the metal complex NHC **29**-AuCl itself could not catalyze the reaction, and the reaction using NHC **29**-AuCl with $AgBF_4$ afforded the product in only 2% ee, indicating that NHC anchoring at the nanoparticle surface is crucial for enantioselectivity.

5 Chiral Diene-Modified Nanoparticle Catalysts

Chiral diene ligands were developed by Hayashi et al. for the first time and were applied for Rh-catalyzed asymmetric reactions [105]. While they initially utilized a bicyclo[2,2,1]heptadiene framework, Carreira et al. concurrently reported other chiral diene ligands with a bicyclo[2,2,2]octadiene framework for Ir-catalyzed asymmetric reactions [106]. Since higher activity of chiral diene-Rh complexes for asymmetric arylation reactions than chiral phosphine Rh complexes was realized, intensive researches of chiral dienes were promoted to develop new structures of chiral dienes and new ligands with hybrid structures including olefins [107–109].

One of the representative applications of chiral diene ligands is asymmetric 1,4-addition of arylboronic acids to unsaturated carbonyl compounds [110, 111]. Thanks to highly active chiral diene Rh complex catalysts, this type of reaction was widely studied to achieve various substrates including not only α,-β-unsaturated carbonyl compounds but also aldehydes, imines, strained alkenes, and alkenyl arenes with excellent enantioselectivities [112]. Not only academic research but also a large-scale (>20 kg) process was demonstrated [113, 114]. However, active, reusable, and robust heterogeneous Rh catalysts for these reactions without metal leaching are demanded because of the high cost of Rh.

In 2012, Kobayashi et al. reported Rh nanoparticle catalysts immobilized on a composite of polystyrene-based copolymer with a cross-linking moiety and carbon black (PI/CB Rh) for asymmetric 1,4-addition of boronic acids to α,β-unsaturated ketones in the presence of a chiral modifier (Scheme 41) [115]. They initially examined chiral phosphine, (*S*)-BINAP **12**, as a chiral modifier for PI/CB Rh; however, a significant amount of Rh leaching was observed during the reaction. On the other hand, the use of a chiral diene as a modifier not only improved catalytic activity and enantioselectivity but also suppress a metal leaching to the detection limit of ICP-AES. Secondly, they examined bimetallic structures to achieve reactions with less reactive acyclic substrates. A bimetallic catalyst consisting of Rh and Ag (PI/CB Rh/Ag) was found to be the most active catalyst, and various enones were

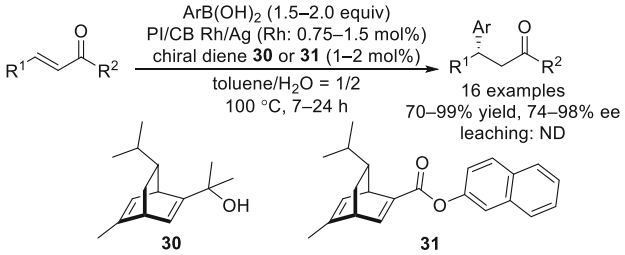

Scheme 41 Chiral diene-modified Rh nanoparticle catalysts for asymmetric 1,4-addition of arylboronic acids to enones

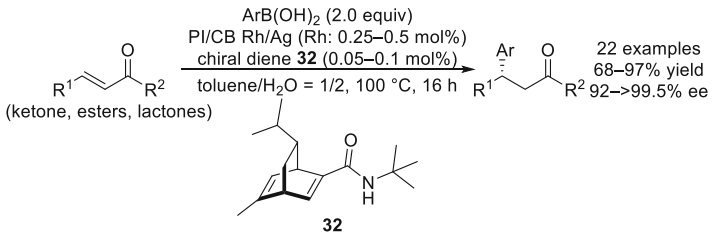

Scheme 42 Secondary amide-substituted chiral diene **32** modified Rh nanoparticle catalysts for asymmetric 1,4-addition of arylboronic acids to unsaturated esters

coupled to the desired α-arylated ketones in high yields with high enantioselectivities in the presence of a chiral modifier **30** or **31** without leaching of the metals. STEM analysis and EDS mapping revealed that alloy nanoparticles formed, and aggregation of Rh nanoparticles was not observed in PI/CB Rh/Ag. PI/CB Rh/Ag could be reused while keeping high yields and high enantioselectivities for 14 times.

In 2015, Kobayashi et al. improved their chiral Rh nanoparticle systems by employing a bifunctional chiral diene bearing a secondary amide moiety (Scheme 42) [116]. The new modifier **32** was supposed to possess a diene part for coordination to metal and a secondary amide group to interact with carbonyl substrates through hydrogen bonding. While the previous chiral diene **30** gave a low enantioselectivity (33% ee) for an asymmetric 1,4-addition to an α,β-unsaturated ester, chiral diene **32**-modified Rh nanoparticle systems dramatically improve the yield and enantioselectivity. Control studies using a tertiary amide-substituted chiral diene that gave a lower enantioselectivity (66% ee) suggested that the secondary amide moiety in diene **32** played an important role in achieving the excellent yield and enantioselectivity. Moreover, the amount of a diene loading could be reduced to 0.05–0.1 mol%, and broad substrate scope including formal synthesis of biologically important compounds was achieved with outstanding enantioselectivities. The Rh catalyst could be reused with the addition of a new portion of the chiral ligand, and no significant loss of the catalytic activity and enantioselectivity was observed over six runs. No metal leaching was confirmed by ICP-AES analysis of the crude

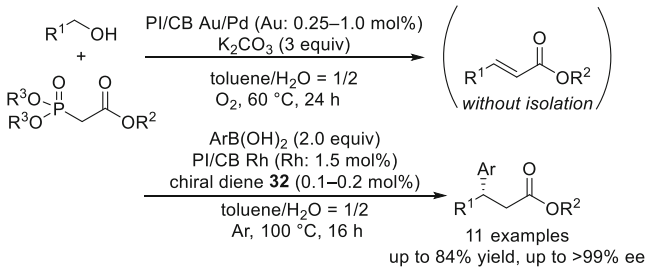

Scheme 43 One-pot oxidation/HWE reaction/asymmetric 1,4-addition reactions catalyzed by Au/Pd nanoparticle and chiral Rh nanoparticle

mixture, and a hot-filtration test confirmed that no reaction proceeded in the filtrate that was obtained in the middle of the reaction.

In this work, several unique natures of Rh nanoparticle systems that were different from the nature of the corresponding homogeneous Rh(I)-diene **32** complex were found. The comparison of the catalytic activity in a homogeneous Rh (I) complex system and the chiral Rh nanoparticle system showed that superior performance of the nanoparticle system in terms of activity and/or enantioselectivity was observed for several substrates. Nonlinear effect analysis [117], which is a plot of enantiopurity of a product against enantiopurity of a chiral ligand, was also conducted in both systems. A positive nonlinear effect was observed in the heterogeneous nanoparticle system, whereas a linear relationship between enantiomeric excess of a ligand and that of a product was observed in the homogeneous metal complex system.

In 2015, Kobayashi et al. applied chiral diene **32**-modified Rh nanoparticle catalysts to an integrated process of oxidation-olefination-asymmetric 1,4-addition reactions (Scheme 43) [118]. Polymer-incarcerated Au/Pd bimetallic catalyst (PI/CB Au/Pd), developed by the authors [119], was used for a tandem process of aerobic oxidation and Horner-Wadsworth-Emmons (HWE) olefination to convert primary alcohols to the corresponding unsaturated esters. After the two-step reaction, PI/CB Rh, arylboronic acid, and chiral diene **32** were added to perform the asymmetric 1,4-addition in the same pot. These three-step, one-pot sequential reactions catalyzed by two different heterogeneous nanoparticle catalysts can produce β-arylated esters in high yields with excellent enantioselectivities from readily available alcohols. Such an integration of reactions has great advantages that can reduce the number of purification steps, and unstable intermediates can be treated in situ.

In the same year, Kobayashi et al. also developed cellulose-supported Rh nanoparticle catalysts for asymmetric 1,4-addition reactions (Scheme 44) [120]. Unlike PI/CB catalysts, Rh nanoparticles were well dispersed over the support without Ag, and this monometallic catalyst showed high catalytic activity in the presence of chiral diene **32** for the reaction with α,β-unsaturated ketones and esters. They analyzed the catalyst with chiral diene **32** by solid-state NMR with the addition of a solvent to swell the sample, so-called swollen-resin magic-angle spinning (SR–MAS) NMR [121]. The pulse sequence consisting of a diffusion filter and isotropic

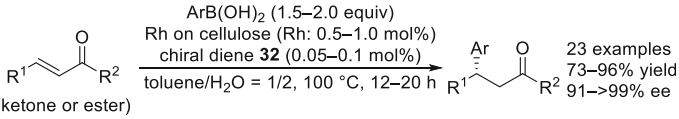

Scheme 44 Cellulose-supported Rh nanoparticle catalysts for asymmetric 1,4-addition reactions

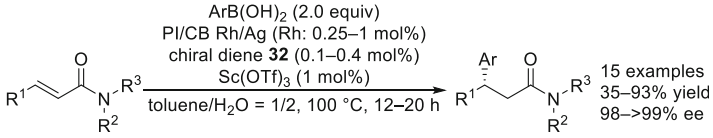

Scheme 45 Cooperative catalyst system using chiral Rh nanoparticle and Lewis acid catalysts for asymmetric 1,4-addition to unsaturated amides

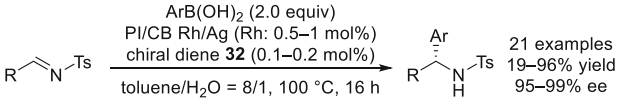

Scheme 46 Chiral Rh nanoparticle catalyzed asymmetric arylation of imines

mixing was used to suppress signals from chiral diene **32** in the solution phase and to exchange the remaining magnetization of cellulose with nearby molecules that would be anchored in the catalyst. The result suggested that the chiral diene **32** adsorbed on the Rh nanoparticles was observed selectively using this method. Similar to the PI/CB Rh/Ag system, a positive nonlinear effect was observed in this cellulose-supported Rh nanoparticle system.

In 2016, Kobayashi et al. reported a cooperative catalyst system using a chiral Rh nanoparticle catalyst and a metal Lewis acid catalyst for asymmetric 1,4-additions to α,β-unsaturated amides (Scheme 45) [122]. α,β-Unsaturated amides are significantly less reactive substrates than α,β-unsaturated ketones and esters because of their high LUMO energy. They employed $Sc(OTf)_3$ as a water-compatible Lewis acidic co-catalyst to activate amide substrates for chiral Rh nanoparticle systems. The reactions proceeded to afford the corresponding β-chiral amides with excellent enantioselectivity without leaching of Rh. The role of $Sc(OTf)_3$ was assumed to lower the LUMO level of the amide substrate to accelerate a C–C bond-forming step and/or accelerate a protonation (product release and catalyst regeneration) step by inner-sphere water ligands of the water-compatible Lewis acid. In the presence of Sc $(OTf)_3$, a higher yield in the heterogeneous nanoparticle catalyst system than that in the corresponding homogeneous Rh-diene **32** complex system was observed, indicating that the heterogeneous nanoparticle catalyst system enhanced the efficiency of the cooperative catalysis.

In 2016, Kobayashi et al. expanded the applicability of chiral Rh nanoparticle systems to asymmetric arylation of aldimines (Scheme 46) [123]. The ratio of

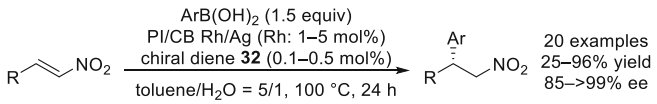

Scheme 47 Chiral Rh nanoparticle catalyzed asymmetric arylation of nitroolefins

toluene and water was optimized to 8:1 to prevent hydrolysis of imines. Asymmetric arylation of aromatic tosylimines proceeded smoothly to afford the corresponding chiral (diarylmethyl)amines in high yields with excellent enantioselectivities in the presence of PI/CB Rh/Ag and chiral diene **32**. On the other hand, as aliphatic imines are more sensitive to water than aromatic imines, the desired products of aliphatic imines were obtained in moderate yields, while enantioselectivities were excellent.

In 2017, Kobayashi et al. further applied chiral Rh nanoparticle systems to asymmetric arylation of nitroolefins (Scheme 47) [124]. The ratio of toluene and water was crucial not only to achieve high yields and enantioselectivities but also to prevent metal leaching. The system worked well even for heteroarene-substituted nitroolefins and aliphatic olefins in excellent enantioselectivity. The nature of active species was discussed in details. First of all, they denied the possibility of the leached homogeneous species as an active species by hot filtration tests. The kinetic behavior of the catalysts recovered at several timings was examined, and their XPS analysis was conducted. These studies suggested a generation of an active species through a redox process between phenyl boronic acid and metal nanoparticles. Considering the similarity of the outcomes of enantioselectivities in homogeneous and heterogeneous systems, they concluded the scenario, in which the reaction proceeded on metal complexes or on very small nanoclusters within the polymer phase, was more likely than the scenario in which the reaction proceeded on the surface of the metal nanoparticles.

6 Other Chiral Molecules as Modifiers

In 2016, Hosseini-Monfared developed magnetite nanoparticles stabilized by L-(+)-tartaric acid (Fe_3O_4/tart-NPs) for asymmetric oxidation of olefins, thioanisole, and tetralin (Scheme 48) [125]. The catalyst was prepared by heating a diethylene glycol solution of $FeCl_3 \cdot 6H_2O$, tartaric acid, and urea at 200°C. Asymmetric oxidation of olefins was performed under oxygen atmosphere in the presence of the catalyst and isobutyl aldehyde as a reductant for the reduction of dioxygen at the beginning of the reaction. Aliphatic substrates gave the corresponding chiral epoxides in moderate to good yields with good to excellent enantioselectivities, while styrene derivatives afforded the products in poor yields and low to moderate enantioselectivities. In the latter case, aldehyde or ketone by-products were observed. The reactions of thioanisole to give the sulfoxide and of tetralin to afford the alcohol also proceeded under the same conditions. The catalysts could be collected by magnetic decantation

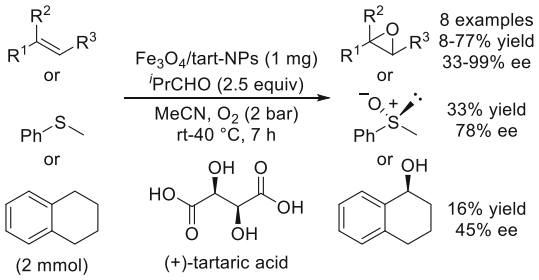

Scheme 48 Asymmetric oxidation of olefins, thioanisole, and tetralin by Fe_3O_4/tart-NPs

and reused five times with increasing catalytic activity after each use in the aerobic oxidation of tetralin.

7 Chiral Polymer-Stabilized Nanoparticle Catalysts

Use of polymer with chiral functionality as a chiral modifier is an attractive subject, as a chiral modifier is expected to be easily recovered. Although silk, as a chiral polymer, supported Pd catalyst was found to be active in asymmetric hydrogenation of benzylidene oxazolidone in the 1950s [3], no successful example of chiral polymer-supported nanoparticle catalysts for asymmetric catalysis was reported until recent studies.

In 2015, Moores et al. utilized cellulose nanocrystals (CNCs) as chiral inducers [126]. Pd nanoparticles were deposited on highly crystalline and well-defined CNCs via treatment of an aqueous mixture of a CNC suspension and a $PdCl_2$ solution under mild H_2 pressure (Scheme 49). Several aromatic ketones were tested as substrates in asymmetric hydrogenation by the Pd nanoparticles on CNCs, and maximally a 65% ee could be obtained from the reaction with *ortho*-methoxy acetophenone (Scheme 50). The aqueous suspension could be recovered by simple phase separation and reused up to three times with no loss of activity and enantioselectivity. The fourth and fifth cycles did lead to a drop in activity, but the enantioselectivity was preserved. Heterogeneity of the catalyst system was also confirmed by a poisoning experiment with CS_2. The 3D structure of the catalyst was studied by cryo-electron microscopy, high-resolution transmission electron microscopy, and tomography. It revealed that sub-nanometer-thick Pd patches are located at the surface of CNCs.

In 2016, Hua et al. reported chiral-substituted poly-*N*-vinylpyrrolidinones (CSPVP **33**) supported bimetallic Pd/Au and Cu/Au nanoparticle catalysts for various asymmetric oxidation reactions [127]. Chiral pyrrolidinone monomers were prepared from *N*-Boc L-(*S*)-amino acids, and the corresponding polymers were used for deposition of bimetallic nanoparticles (Scheme 51). Various structures of monomers were examined in asymmetric oxidation of 1,3-diol, and CSPVP **33** was found to be the best chiral inducer. Pd/Au bimetallic nanoparticle catalysts on CSPVP **33** were applied to kinetic resolution of *trans*-1,2 and 1,3-diols and asymmetric mono oxidation of *cis*-1,2 and 1,3-diols to produce the corresponding

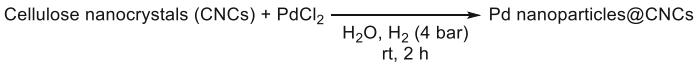

Scheme 49 Preparation of cellulose nanocrystals supported Pd nanoparticles

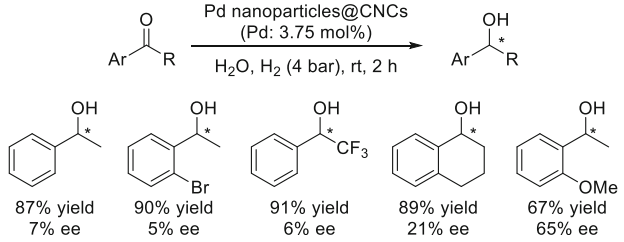

Scheme 50 Pd nanoparticles on CNCs catalyzed asymmetric hydrogenation of ketones

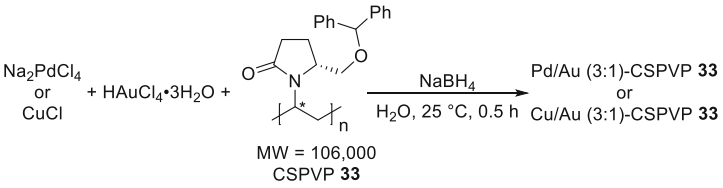

Scheme 51 Preparation of chiral-substituted poly-*N*-vinylpyrrolidinones **33** supported bimetallic catalysts

hydroxy ketones in excellent enantioselectivity (Scheme 52). The same catalyst was also utilized for asymmetric oxidation of alkenes to afford diols with excellent enantioselectivities (Scheme 53). Interestingly, resulting diols did not undergo further oxidation even though benzylic alcohols were easily oxidized by Au nanoparticle catalysts [128]. Furthermore, Cu/Au bimetallic nanoparticle catalysts on CSPVP **33** were applied to asymmetric C–H oxidation of cycloalkanes to produce ketones with excellent enantioselectivities (Scheme 54).

In 2017, Chen and Dong et al. reported Pd nanoparticles loaded on a homochiral covalent organic framework (COF) for asymmetric catalysis [129]. The chiral COF support (CCOF-MPC) was synthesized from cyanuric chloride and *S*-(+)-2-methylpiperazine at 90°C, and the Pd nanoparticles were loaded on CCOF-MPC via sequential solution impregnation and reduction of a Pd salt by $NaBH_4$ to afford the catalyst (Pd@CCOF-MPC) (Scheme 55). High-resolution transmission electron microscopy (HRTEM) analysis of the catalyst showed highly dispersed Pd nanoparticles with a particle size of 2–5 nm. The size of the Pd nanoparticles was larger than that of the pore size (1.5 nm) in Pd@CCOF-MPC indicating that Pd nanoparticles might be located between the 2D COF layers. An increase in the interlayer spacing of COF was also demonstrated by the PXRD pattern of the catalyst.

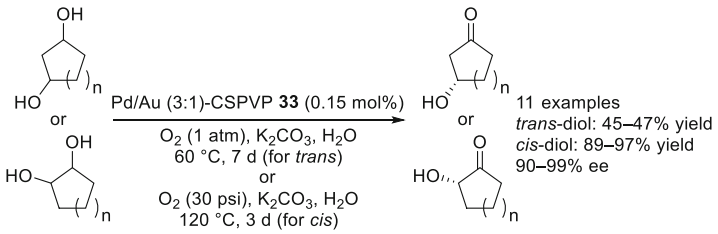

Scheme 52 Pd/Au-CSPVP **33** catalyzed asymmetric oxidation of 1,3-diols and 1,2-diols

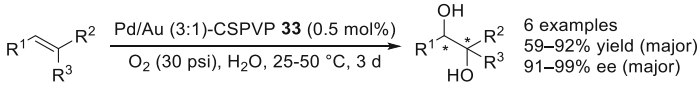

Scheme 53 Pd/Au-CSPVP **33** catalyzed asymmetric oxidation of alkenes

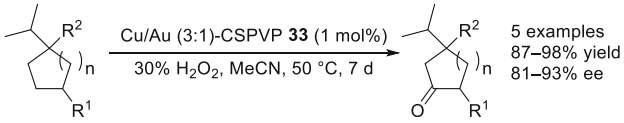

Scheme 54 Cu/Au-CSPVP **33** catalyzed asymmetric oxidation of cycloalkanes

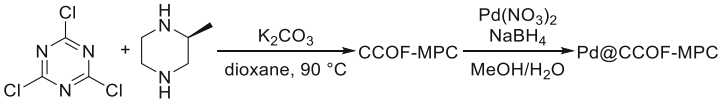

Scheme 55 Preparation of Pd@CCOF-MPC

Pd@CCOF-MPC was applied to asymmetric Henry reactions, and various aromatic aldehydes were converted to the corresponding β-nitro alcohols in high enantioselectivity (Scheme 56). CCOF-MPC itself hardly catalyzed the reaction indicating that Pd nanoparticles in the CCOF-MPC matrix are responsible for the catalytic activity. The catalyst was also applied to asymmetric reductive Heck reactions of 2-cyclohexen-1-one with aryl halides (Scheme 57). Although Pd nanoparticles were aggregated and leached out after five runs in both reactions, relatively high levels of yield and enantioselectivity were maintained.

In 2017, Sharma et al. reported Pt nanoparticles incorporated chiral polyamide for asymmetric hydrogenation of an α-ketoester [130]. Chiral polyamides were synthesized from camphoric dichloride and diamine monomers by interfacial condensation reactions. A Pt(IV) salt was loaded on the polymer followed by reduction under high-pressure hydrogen to afford the catalyst, Pt(0)/chiral polyamide (Scheme 58). Several diamine linkers were examined, and the catalyst prepared from hexamethylenediamine showed the best performance in asymmetric hydrogenation

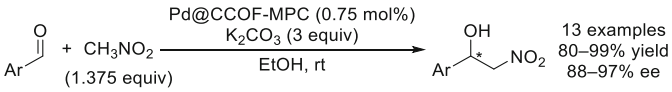

Scheme 56 Pd@CCOF-MPC catalyzed asymmetric Henry reaction

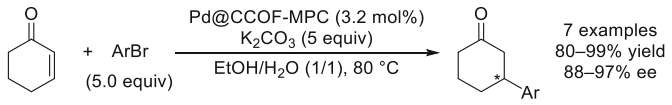

Scheme 57 Pd@CCOF-MPC catalyzed asymmetric reductive Heck reaction

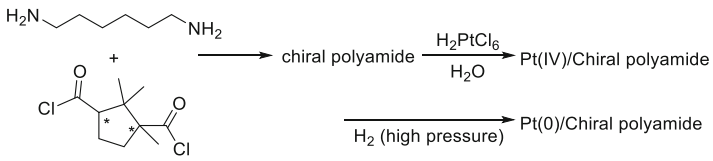

Scheme 58 Preparation of chiral polyamide supported Pt nanoparticle catalysts

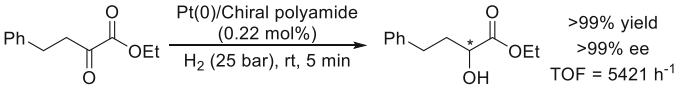

Scheme 59 Pt(0)/chiral polyamide catalyzed asymmetric hydrogenation of ethyl 2-oxo-4-phenylbutanoate

of ethyl 2-oxo-4-phenylbutanoate with excellent enantioselectivity (Scheme 59). The catalyst could be reused for ten cycles with slight loss of enantioselectivity. This chiral polyamide supports have helical structure with molecular chirality examined by the CD and UV-vis spectroscopies.

8 Conclusion

As introduced in this chapter, chiral nanoparticle catalytic systems have a potential to construct robust asymmetric catalysts. Thanks to diverse choice of chiral modifiers, which were originally used for homogeneous metal complex catalysis, applicable reactions catalyzed by chiral metal nanoparticles were dramatically expanded especially since 2000. Several reports proved that not only small molecules but also chiral polymers would be good candidates of chiral modifiers for nanoparticles. Some examples demonstrated excellent enantioselectivities with broad substrate generality and reusability, and they must be useful heterogeneous catalysts. Moreover, chiral metal nanoparticles showed unique catalytic behaviors that are different from the corresponding homogeneous metal complex systems. It indicates that the

active species in nanoparticle catalysis are not leached molecular complexes although true active species are unclear in most cases. This is an emerging area of research, and we expect that further studies lead to achievement of more efficient and unique chiral nanoparticle catalysis.

References

1. Ojima I (2010) Catalytic asymmetric synthesis. Wiley, Hoboken
2. Christmann M, Bräse S (2012) Asymmetric synthesis II: more methods and applications. Wiley, Hoboken
3. Akabori S, Sakurai S, Izumi Y, Fujii Y (1956) Nature 178:323
4. Izumi Y, Imaida M, Fukawa H, Akabori S (1963) Bull Chem Soc Jpn 36:21
5. Izumi Y, Imaida M, Fukawa H, Akabori S (1963) Bull Chem Soc Jpn 36:155
6. Tatsumi S, Imaida M, Fukuda Y, Izumi Y, Akabori S (1964) Bull Chem Soc Jpn 37:846
7. Orito Y, Imai S, Niwa S (1979) Nippon Kagaku Kaishi:1118
8. Orito Y, Imai S, Niwa S, Nguyen GH (1979) J Synth Org Chem Jpn 37:173
9. Rodríguez-García L, Hungerbühler K, Baiker A, Meemken F (2017) ACS Catal 7:3799
10. Xue XR, Wang YH, Han FS (2017) Chem Commun 53:3346
11. Yang T, Lou LL, Yu WJ, Feng YJ, Li H, Yu K, Liu SX (2017) ChemCatChem 9:458
12. Mao C, Zhang J, Xiao MT, Liu YJ, Zhang XQ (2018) Curr Appl Phys 18:1480
13. Meemken F, Rodriguez-Garcia L (2018) J Phys Chem Lett 9:996
14. Xue XR, Chen P, Xu P, Wang YH (2018) Catal Commun 110:55
15. Xue XR, Zhao ZH, Wang YH (2018) Org Chem Front 5:3585
16. Blaser H-U, Studer M (2007) Acc Chem Res 40:1348
17. Zhan E, Chen C, Li Y, Shen W (2015) Cat Sci Technol 5:650
18. Baiker A (2015) Chem Soc Rev 44:7449
19. Meemken F, Baiker A (2017) Chem Rev 117:11522
20. Tang Z (2018) Chiral nanomaterials: preparation, properties and applications. Wiley, Hoboken
21. Maeda N, Hungerbühler K, Baiker A (2011) J Am Chem Soc 133:19567
22. Meemken F, Maeda N, Hungerbuehler K, Baiker A (2012) Angew Chem Int Ed 51:8212
23. Goubert G, McBreen PH (2013) ChemCatChem 5:683
24. Crabtree RH (2012) Chem Rev 112:1536
25. Demers-Carpentier V, Goubert G, Masini F, Lafleur-Lambert R, Dong Y, Lavoie S, Mahieu G, Boukouvalas J, Gao H, Rasmussen AMH, Ferrighi L, Pan Y, Hammer B, McBreen PH (2011) Science 334:6057
26. Orglmeister E, Mallat T, Baiker A (2005) Adv Synth Catal 347:78
27. Dong Y, Svane K, Lemay JC, Groves MN, McBreen PH (2017) ACS Catal 7:1757
28. Goubert G, Dong Y, Groves MN, Lemay JC, Hammer B, McBreen PH (2017) Nat Chem 9:531
29. Lavoie S, Laliberté M-A, Temprano I, McBreen PH (2006) J Am Chem Soc 128:7588
30. Studer M, Burkhardt S, Blaser H-U (1999) Chem Commun:1727
31. von Arx M, Mallat T, Baiker A (2002) Catal Lett 78:267
32. Diezi S, Hess M, Orglmeister E, Mallat T, Baiker A (2005) Catal Lett 102:121
33. Yang HP, Wang H, Lu JX (2015) Electrochem Commun 55:18
34. Yang HP, Fen Q, Wang H, Lu JX (2016) Electrochem Commun 71:38
35. Yue YN, Wu D, Zeng S, Yang MP, Wang H, Lu JX (2017) New J Chem 41:7853
36. Zhu J, Sun X-T, Wang X-D, Wu L (2018) ChemCatChem 10:1788
37. Tungler A, Tarnai T, Máthé T, Petró J (1991) J Mol Catal 67:277
38. Perosa A, Tundo P, Selva M (2002) J Mol Catal A Chem 180:169
39. Vetere V, Faraoni MB, Santori GF, Podestá J, Casella ML, Ferretti OA (2004) J Catal 226:457

40. Vetere V, Faraoni MB, Santori GF, Podestá JC, Casella ML, Ferretti OA (2005) Catal Today 107–108:266
41. Cheng H, Hao J, Wang H, Xi C, Meng X, Cai S, Zhao F (2007) J Mol Catal A Chem 278:6
42. Wang J, Feng H, Qin R, Fu H, Yuan M, Chen H, Li X (2007) Tetrahedron Asymmetry 18:1643
43. Jiang HY, Yang CF, Li C, Fu HY, Chen H, Li RX, Li XJ (2008) Angew Chem Int Ed 47:9240
44. Jiang H-Y, Sun B, Zheng X-X, Chen H (2012) Appl Catal A 421:86
45. Li C, Zhang L, Zheng C, Zheng X, Fu H, Chen H, Li R (2014) Tetrahedron Asymmetry 25:821
46. Yang CF, Jiang HY, Feng J, Fu HY, Li RX, Chen H, Li XJ (2009) J Mol Catal A Chem 300:98
47. Li C, Zhang L, Liu H, Zheng X, Fu H, Chen H, Li R (2014) Catal Commun 54:27
48. Jiang H-Y, Chen H, Li R-X (2010) Catal Commun 11:584
49. Tungler A, Kajtar M, Mathe T, Toth G, Fogassy E, Petro J (1989) Catal Today 5:159
50. Tungler A, Máthé T, Petró J, Tarnai T (1990) J Mol Catal 61:259
51. McIntosh AI, Watson DJ, Burton JW, Lambert RM (2006) J Am Chem Soc 128:7329
52. Mhadgut SC, Török M, Dasgupta S, Török B (2008) Catal Lett 123:156
53. Watson DJ, Jesudason RJBRJ, Beaumont SK, Kyriakou G, Burton JW, Lambert RM (2009) J Am Chem Soc 131:14584
54. Mhadgut SC, Török M, Esquibel J, Török B (2006) J Catal 238:441
55. Schafer C, Mhadgut SC, Kugyela N, Torok M, Torok B (2015) Cat Sci Technol 5:716
56. Rodríguez-García L, Hungerbühler K, Baiker A, Meemken F (2015) J Am Chem Soc 137:12121
57. Kunz S, Schreiber P, Ludwig M, Maturi MM, Ackermann O, Tschurl M, Heiz U (2013) Phys Chem Chem Phys 15:19253
58. Schrader I, Warneke J, Backenköhler J, Kunz S (2015) J Am Chem Soc 137:905
59. Schrader I, Neumann S, Himstedt R, Zana A, Warneke J, Kunz S (2015) Chem Commun 51:16221
60. Schrader I, Neumann S, Sulce A, Schmidt F, Azov V, Kunz S (2017) ACS Catal 7:3979
61. Šulce A, Backenköhler J, Schrader I, Piane MD, Müller C, Wark A, Ciacchi LC, Azov V, Kunz S (2018) Cat Sci Technol 8:6062
62. Gross E, Liu JH, Alayoglu S, Marcus MA, Fakra SC, Toste FD, Somorjai GA (2013) J Am Chem Soc 135:3881
63. Tang W, Zhang X (2003) Chem Rev 103:3029
64. Li YM, Kwong FY, Yu WY, Chan ASC (2007) Coord Chem Rev 251:2119
65. Pereira MM, Calvete MJF, Carrilho RMB, Abreu AR (2013) Chem Soc Rev 42:6990
66. Mikhailine A, Lough AJ, Morris RH (2009) J Am Chem Soc 131:1394
67. Meyer N, Lough AJ, Morris RH (2009) Chem Eur J 15:5605
68. Sonnenberg JF, Morris RH (2014) Cat Sci Technol 4:3426
69. Sonnenberg JF, Coombs N, Dube PA, Morris RH (2012) J Am Chem Soc 134:5893
70. Prokopchuk DE, Sonnenberg JF, Meyer N, Zimmer-De Iuliis M, Lough AJ, Morris RH (2012) Organometallics 31:3056
71. Li Y, Yu S, Wu X, Xiao J, Shen W, Dong Z, Gao J (2014) J Am Chem Soc 136:4031
72. Cano I, Tschan MJL, Martinez-Prieto LM, Philippot K, Chaudret B, van Leeuwen P (2016) Cat Sci Technol 6:3758
73. Xia YT, Ma J, Wang XD, Yang L, Wu L (2017) Cat Sci Technol 7:5515
74. Riant O, Mostefai N, Courmarcel J (2004) Synthesis:2943
75. Tamura M, Fujihara H (2003) J Am Chem Soc 125:15742
76. Kantam ML, Laha S, Yadav J, Likhar PR, Sreedhar B, Choudary BM (2007) Adv Synth Catal 349:1797
77. Kantam ML, Yadav J, Laha S, Srinivas P, Sreedhar B, Figueras F (2009) J Org Chem 74:4608
78. Li M, Li B, Xia H-F, Ye D, Wu J, Shi Y (2014) Green Chem 16:2680
79. Akiyama R, Kobayashi S (2001) Angew Chem Int Ed 40:3469
80. Jansat S, Gómez M, Philippot K, Muller G, Guiu E, Claver C, Castillon S, Chaudret B (2004) J Am Chem Soc 126:1592

81. Favier I, Gómez M, Muller G, Axet MR, Castillon S, Claver C, Jansat S, Chaudret B, Philippot K (2007) Adv Synth Catal 349:2459
82. Dieguez M, Pamies O, Mata Y, Teuma E, Gomez M, Ribaudo F, van Leeuwen PWNM (2008) Adv Synth Catal 350:2583
83. Felpin FX, Landais Y (2005) J Org Chem 70:6441
84. Reimann S, Mallat T, Baiker A (2007) J Catal 252:30
85. Reimann S, Mallat T, Baiker A (2008) J Catal 254:79
86. Reimann S, Grunwaldt J-D, Mallat T, Baiker A (2010) Chem Eur J 16:9658
87. Sawai K, Tatumi R, Nakahodo T, Fujihara H (2008) Angew Chem Int Ed 47:6917
88. Mori K, Kondo Y, Yamashita H (2009) Phys Chem Chem Phys 11:8949
89. Klosin J, Landis CR (2007) Acc Chem Res 40:1251
90. Neves ACB, Calvete MJF, Melo T, Pereira MM (2012) Eur J Org Chem:6309
91. Coronado JM, Coloma F, Anderson JA (2000) J Mol Catal A Chem 154:143
92. Han D, Li X, Zhang H, Liu Z, Li J, Li C (2006) J Catal 243:318
93. Han D, Li X, Zhang H, Liu Z, Hu G, Li C (2008) J Mol Catal A Chem 283:15
94. Axet MR, Castillon S, Claver C, Philippot K, Lecante P, Chaudret B (2008) Eur J Inorg Chem 2008:3460
95. Alsalahi W, Trzeciak AM (2018) ChemistrySelect 3:1727
96. Park KH, Chung YK (2005) Adv Synth Catal 347:854
97. Chen MY, Xu Z, Chen L, Song T, Zheng ZJ, Cao J, Cui YM, Xu LW (2018) ChemCatChem 10:280
98. Hopkinson MN, Richter C, Schedler M, Glorius F (2014) Nature 510:485
99. Zhukhovitskiy AV, MacLeod MJ, Johnson JA (2015) Chem Rev 115:11503
100. Ranganath KVS, Kloesges J, Schäfer AH, Glorius F (2010) Angew Chem Int Ed 49:7786
101. Richter C, Ranganath KVS, Glorius F (2012) Adv Synth Catal 354:377
102. Ranganath KVS, Schaefer AH, Glorius F (2011) ChemCatChem 3:1889
103. Ye R, Zhukhovitskiy AV, Kazantsev RV, Fakra SC, Wickemeyer BB, Toste FD, Somorjai GA (2018) J Am Chem Soc 140:4144
104. Shu X-Z, Nguyen SC, He Y, Oba F, Zhang Q, Canlas C, Somorjai GA, Alivisatos AP, Toste FD (2015) J Am Chem Soc 137:7083
105. Hayashi T, Ueyama K, Tokunaga N, Yoshida K (2003) J Am Chem Soc 125:11508
106. Fischer C, Defieber C, Suzuki T, Carreira EM (2004) J Am Chem Soc 126:1628
107. Defieber C, Gruetzmacher H, Carreira EM (2008) Angew Chem Int Ed 47:4482
108. Dong HQ, Xu MH, Feng CG, Sun XW, Lin GQ (2015) Org Chem Front 2:73
109. Nagamoto M, Nishimura T (2017) ACS Catal 7:833
110. Hayashi T, Yamasaki K (2003) Chem Rev 103:2829
111. Takaya Y, Ogasawara M, Hayashi T, Sakai M, Miyaura N (1998) J Am Chem Soc 120:5579
112. Tian P, Dong H-Q, Lin G-Q (2012) ACS Catal 2:95
113. Howell GP (2012) Org Process Res Dev 16:1258
114. Brock S, Hose D, Moseley J, Parker A, Patel I, Williams A (2008) Org Process Res Dev 12:496
115. Yasukawa T, Miyamura H, Kobayashi S (2012) J Am Chem Soc 134:16963
116. Yasukawa T, Suzuki A, Miyamura H, Nishino K, Kobayashi S (2015) J Am Chem Soc 137:6616
117. Satyanarayana T, Abraham S, Kagan HB (2009) Angew Chem Int Ed 48:456
118. Miyamura H, Suzuki A, Yasukawa T, Kobayashi S (2015) Adv Synth Catal 357:3815
119. Kobayashi S, Miyamura H (2013) Aldrichimica Acta 46:3
120. Yasukawa T, Miyamura H, Kobayashi S (2015) Chem Sci 6:6224
121. Kobayashi S, Akiyama R, Furuya T, Moriwaki M (1998) Molecules 2:35
122. Yasukawa T, Saito Y, Miyamura H, Kobayashi S (2016) Angew Chem Int Ed 55:8058
123. Yasukawa T, Kuremoto T, Miyamura H, Kobayashi S (2016) Org Lett 18:2716
124. Miyamura H, Nishino K, Yasukawa T, Kobayashi S (2017) Chem Sci 8:8362
125. Hadian-Dehkordi L, Hosseini-Monfared H (2016) Green Chem 18:497

126. Kaushik M, Basu K, Benoit C, Cirtiu CM, Vali H, Moores A (2015) J Am Chem Soc 137:6124
127. Hao B, Gunaratna MJ, Zhang M, Weerasekara S, Seiwald SN, Nguyen VT, Meier A, Hua DH (2016) J Am Chem Soc 138:16839
128. Takale BS, Bao M, Yamamoto Y (2014) Org Biomol Chem 12:2005
129. Ma HC, Kan JL, Chen GJ, Chen CX, Dong YB (2017) Chem Mater 29:6518
130. Sharma P, Sharma RK (2017) ChemistrySelect 2:513